Journal of Engineering and Technology for Industrial Applications

ITEGAM-JETIA

Manaus, v.11 n.52, p. 103-111. March / April, 2025.

DOI: https://doi.org/10.5935/jetia.v11i52.1550

ISSN ONLINE: 2447-0228

RESEARCH ARTICLE OPEN ACCESS

INCORPORATING ANFIS BASED CURRENT REGULATION INTO A MULTI ACTIVE FULL BRIDGE CONVERTER FOR REDUCING CURRENT RIPPLE

Rathod Rama Krishna[1], G. Yesuratnam[2] and Dr. Punnaiah Veeraboina[3]

[1]Department of Electrical Engineering, University College of Engineering, Osmania University, Hyderabad, Telangana 500007, India
[2]Senior Professor, Department of Electrical Engineering, University College of Engineering, Osmania University, Hyderabad, Telangana, India
[3]Electrical Engineering Section, Engineering Department, BRIC-CDFD, Minister of Science and Technology, Govt of India

[1]http://orcid.org/0009-0002-4669-3124, [2]http://orcid.org/0000-0002-4730-4496, [3]http://orcid.org/0000-0001-9158-4109

Email: rathodkrishnaou@osmania.ac.in, ratnamgy@uceou.edu, drveera33@gmail.com

ARTICLE INFO

Article History
Received: January 11, 2025
Revised: February 20, 2025
Accepted: March 15, 2025
Published: March 31, 2025

Keywords:
Zero Voltage Switching (ZVS),
Zero Current Switching (ZCS),
Electric Vehicle (EV),
PI (Proportional and Integral),
Adaptive Neuro Fuzzy Inference System (ANFIS)

ABSTRACT

A multi-active full bridge converter is a type of DC-DC converter typically used in high-power applications like renewable energy systems, electric vehicles, or uninterruptible power supplies. Four switches (often MOSFETs or IGBTs) grouped in an H-bridge configuration make up the full bridge topology. The term "multi-active" implies that the power conversion involves a number of active components, which may indicate complicated switching management for improved efficiency and regulation. Changing the phase shift between two switch pairs is how phase-shifted full-bridge converters are controlled. Without altering the switching frequency, the output voltage can be controlled by adjusting the phase difference between the bridge's two legs (S1-S4 and S2-S3). To lower switching losses, soft switching strategies like ZVS or ZCS might be used. improving overall efficiency. In this approach, the current through the switches is monitored and controlled to improve transient response and stability. Typically implemented in combination with voltage mode control, it ensures better regulation, especially in systems with fast load changes. The secondary side full bridge switches are controlled by current feedback phase delay controller which restricts the battery charge current. Each EV battery has its own charge current limit which is set in the current controller for battery protection. The controlled charge current improves the charge efficiency of the EV battery increasing the reliability of the cells and the overall circuit. The charge control which is a conventional PI controller is further updated with ANFIS for better stability in the EV battery charging current. A comparative analysis with PI and ANFIS controllers is proposed and the results are generated with same rating of EV batteries and system parameters.

I. INTRODUCTION

As per the present climatic conditions we are at verge of crossing temperature limits due to global warming caused by carbon emissions. The carbon emissions are majorly caused by the industrial manufacturing plants which need to be limited. Another major reason for the emissions is transportation using fossil fuel vehicles for domestic and commercial purposes [1].

The utilization of petrol or diesel engines in the vehicles is leading to extreme climatic conditions causing health issues for all the living beings on the planet. It is very vital to replace these vehicles with zero carbon emission vehicles which run on complete electrical power. This can be achieved by electrical vehicles (EVs) which operate by electrical motor drive. The electrical motor receives power from mobile battery pack (combination of several battery cells) which need to be charged [2]. Charging the EV battery pack using conventional power generation sources like coal plants or diesel generators is considered to be futile [3]

Therefore, these battery packs need to be charged using renewable sources like solar generation plants, wind farms, bio gas plants, tidal energy etc. The renewable sources are inter

connected to the conventional grid which shares power to the local loads or EV charging stations or to the other grid network as per the demand [4]. Grid interconnection of renewable sources creates stable operation of the network as the renewable sources are unpredictable. However, in remote areas the grid availability cannot be expected as the transmission lines may not reach some localities.

Therefore, backup storage devices need to be installed along with the renewable sources for voltage and power stability [5]. High capacity back up storage devices like battery modules are associated with the renewable source for storing or providing power as per requirement. A local load is connected to this network with an inverter operated by Sin PWM technique to ensure Sinusoidal AC generation from the DC power generated by the PV plant and battery storage module.

The load connected to the inverter is a static load which is operated at fundamental AC frequency of 50Hz [6]. At the DC common link an EV charging station is connected with multiple charging points for charging several EVs. The complete structure with standalone PV plant with battery storage module and EV charging station is presented in figure 1.

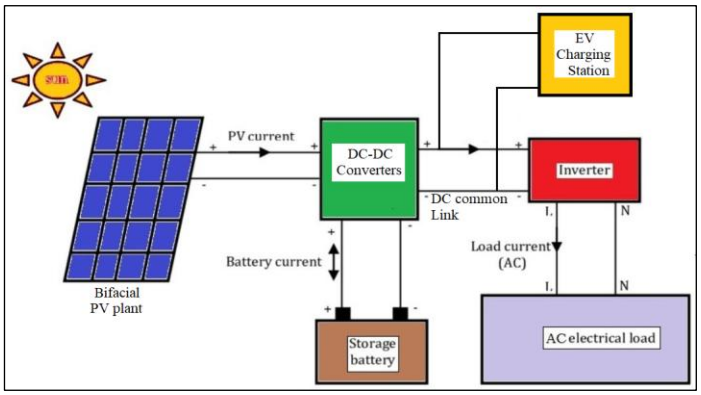

Figure 1: Outline structure of standalone PV plant with EV charging station.
Source: Authors, (2025).

As presented in figure 1 the PV plant and battery storage are connected to DC-DC converters for power delivery and exchange. The PV plant uses 'Bifacial PV module' which has two panels connected back-to-back for more power generation than the conventional PV plant. The back panels have the capability to generate 20% extra PV power by the solar radiation reflection [7]. The Bifacial PV panels are connected to boost converter operated by MPPT controller for maximum power extraction from the panels.

The storage battery module is connected to a bidirectional converter with power exchanging capabilities as per the demand and availability. The AC electrical load is a fixed value static load feeding from the DC common link. The EV charging station connected at the DC common link has Multi Active Full Bridge (MAFB) converter exchanging power between the DC common link and EV batteries [8].

The MAFB has the capability to operate in G2V (Grid to Vehicle) and V2G (Vehicle to Grid) modes as per the requirement. The charging and discharging currents of the MAFB converter circuit is controlled by individual current regulators. The MAFB is operated by phase shift pulse modulation (PS-PM) technique which creates phase delay in the pulses of the active switches of the full bridges [9]. The phase delay value in the PS-PM technique is generated by the current regulator integrated in the controller. Initially the current regulator considered is a PI regulator which has more damping. Due to the heavy damping in PI regulator, the battery currents have more oscillations and ripple. Therefore, the PI regulator is replaced with ANFIS current regulator with optimal damping creating robust phase shift signal for the switches. This reduces the oscillations and ripple in the battery currents [10].

This paper is organized with introduction to the proposed structure of the PV standalone system with EV charging station in section 1. The section 2 is included with configuration of the complete system with design of the circuits and controllers used for the stabilization of the system. The EV charging module MAFB converter circuit with PI and ANFIS current regulators designs are discussed in section 3. The following section 4 has the results analysis of the simulations designed and modelled operating in different operating conditions. A simulation comparative analysis is presented in this section 4 followed by conclusion in section 5 validating the optimal controller. The references cited in the paper are included at the end of the paper after section 5.

II. CONFIGURATION PROOSED SYSTEM

As previously mentioned, charging the EV battery packs by the conventional fossil fuel sources is futile. Therefore, renewable sources need to be installed in the system operating in standalone mode. In the proposed system a standalone PV source is installed for sharing power to the local load and EV charging station for charging the battery pack with renewable power. The PV sources use Bifacial PV panels for extra renewable power generation with the same solar irradiation.

Due to the Bifacial structure of the PV panels a 20% extra power is generated from the PV plant. Bifacial PV arrays are solar panels capable of generating electricity from sunlight on both their front and rear sides [11]. These panels capture sunlight directly on the front while also utilizing reflected or diffused light on the rear. As a result, bifacial PV panels can produce more electricity per panel, particularly in environments with high albedo, such as snowy areas, sandy locations, or on white roofs.

Bifacial solar panels can achieve 10–30% more energy output compared to traditional single-faced panels, depending on installation and the albedo (reflectivity) of the ground surface [12]. This increased energy generation per panel reduces the overall cost of electricity over the system's lifetime, allowing for fewer panels or less land to achieve the same energy output as single-faced systems. Many bifacial panels are constructed with glass on both sides, which makes them more durable and resistant to environmental stressors such as humidity, UV radiation, and mechanical loads.

As a result, they tend to degrade more slowly over time, ensuring consistent performance. Bifacial panels can be effectively used in various applications, including carports, pergolas, or other elevated structures where the rear side can receive significant reflected or diffused light [13]. They also perform well under cloudy conditions or in areas with considerable diffused sunlight, as both sides of the panel can contribute to energy generation.

Standalone photovoltaic (PV) systems, also known as off-grid solar systems, operate independently of the utility grid. While they provide a clean and renewable energy source, they also have some drawbacks and challenges [14]. These systems are typically designed to meet a specific energy demand. If energy consumption exceeds the system's capacity, upgrades will be necessary. Users must manage their energy use carefully to avoid

overloading the system, particularly during peak consumption times.

To ensure reliable performance throughout the year, standalone systems are often oversized, which can lead to higher initial costs and potential energy waste during peak sunlight periods [15]. Additionally, these systems are generally not suitable for powering high-energy equipment or industrial applications without significant scaling. To maintain consistent power availability, standalone systems require batteries to store energy generated during sunny periods and provide power during times of lower generation. The circuit structure of the PV panels standalone system with battery storage backup feeding the local load and EV charging station is presented in figure 2.

As observed in figure 2, Bifacial PV array is connected to single switch boost converter which is operated using P&O MPPT technique [16]. The duty ratio of the switch is changed as per the voltage and current of the Bifacial PV array which is dependent on solar irradiation. The change in duty ratio is given as:

$$D(n) = D(n-1) + \int \Delta D \begin{cases} If\ Ppv(n) > Ppv(n-1)\ and\ Vpv(n) > Vpv(n-1) \\ If\ Ppv(n) < Ppv(n-1) amd\ Vpv(n) < Vpv(n-1) \end{cases} \quad (1)$$

$$D(n) = D(n-1) - \int \Delta D \begin{cases} If\ Ppv(n) < Ppv(n-1)\ and\ Vpv(n) > Vpv(n-1) \\ If\ Ppv(n) > Ppv(n-1) amd\ Vpv(n) < Vpv(n-1) \end{cases} \quad (2)$$

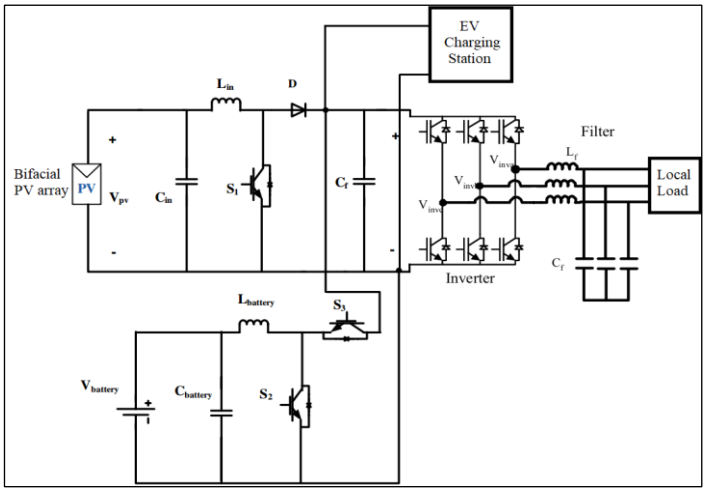

Figure 2: Circuit structure of standalone PV source with battery backup storage.
Source: Authors, (2025).

The previous duty ratio $D(n-1)$ is updated by an integrated ΔD value either adding or subtracting the previous duty ratio. Here, $Ppv(n)$ and $Ppv(n-1)$ are the present and previous values of Bifacial PV array power. $Vpv(n)$ and $Vpv(n-1)$ are the present and previous values of Bifacial PV array voltage.

On the other hand, the battery storage is connected to bidirectional converter with two switches connected in the circuit [17]. These two switches are operated alternatively using voltage regulator controller. This voltage regulator controller maintains the DC common link voltage at specified reference value for stability system voltages [18]. The voltage regulator controller for the battery storage circuit is presented in figure 3.

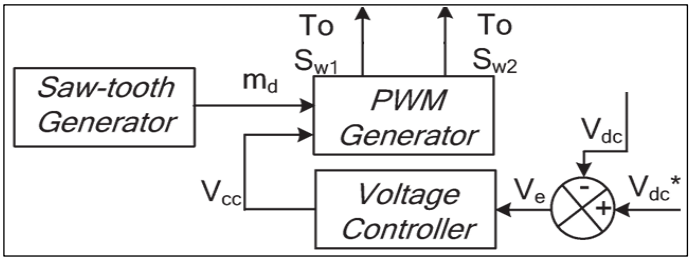

Figure 3: Voltage regulator controller.
Source: Authors, (2025).

As per figure 3, the reference DC common link voltage (Vdc*) are compared to measured DC link voltage generating error voltage (Ve). The Ve signal is given to voltage regulator controller to generate duty ratio (Vcc) of the switch S_{w1}. The Vcc is compared to sawtooth generator for generating pulses to the S_{w1} and the NOT gate signal is set to S_{w2}. Here, the voltage regulator controller is PI controller with tuned K_{pdc} and K_{idc} (Proportional and Integral) gains set as per the DC common link voltage stability [19]. The duty ration Vcc is given as:

$$V_{cc} = (V_{dc}^{*} - V_{dc})\left(K_{pdc} + \frac{K_{idc}}{s}\right) \quad (3)$$

The stabilized DC common link voltage is fed to three phase inverter converting DC to three phase AC feeding the local load. The three-phase inverter is controlled by Sin PWM technique which generates pulses to the switches by comparing three phase Sinusoidal signals with high frequency triangular waveform.

III. MAFB CONTROL DESIGN

In the proposed system the EV charging station connected at the DC common link has multiple bidirectional converters [20]. The conventional bidirectional converter with two switches has very high-power loss, high ripple and lesser efficiency. This converter is replaced with dual active full bridge converters for better efficiency, less ripple and reduced power loss.

As the dual active full bridge converter has single input and single output terminals, several converters need to be connected individually to each EV battery for exchanging power. This increases the number of components in the charging station which leads to initial installation cost. Therefore, multiple dual active full bridge circuits are replaced with a single Multi active full bridge (MAFB) topology with single input and multi output terminals [21].

A MAFB topology is a type of DC-DC power converter that is widely used in high-power applications, including renewable energy systems, electric vehicle chargers, uninterruptible power supplies (UPS), and industrial power systems. This design is based on the conventional full-bridge topology but incorporates advanced techniques to enhance efficiency, reduce losses, and facilitate bidirectional power transfer. This makes it particularly useful in systems like battery storage, where energy needs to flow in both directions for charging and discharging.

The basic topology consists of four active switches, typically MOSFETs or IGBTs, arranged in a full-bridge structure. These switches alternate between on and off states to generate a high-frequency AC signal [22]. A High-Frequency Transformer (HFT) is employed to provide galvanic isolation between the input and output, while also allowing for voltage scaling (either stepping up or stepping down) based on the turns ratio.

The converter is capable of operating in both rectification and inversion modes, making it ideal for systems like energy storage, where power must flow in either direction. Techniques such as Zero Voltage Switching (ZVS) and Zero Current Switching (ZCS) are utilized to minimize switching losses and enhance overall efficiency, particularly at high frequencies.

The converter can incorporate advanced control strategies like PS-PM to achieve precise regulation of output voltage and current [23]. The MAFB is a versatile and efficient solution that meets the growing demand for high-performance and reliable power converters in modern applications. Its ability to manage bidirectional power flow and maintain high efficiency makes it a foundational technology in the field of power electronics. The circuit of the MAFB topology connected at the DC common link of the standalone system is shown in figure 4.

The input DC voltage is applied to a full-bridge circuit, which is made up of four active switches (either MOSFETs or IGBTs) arranged in an "H" configuration. By alternately turning these switches on and off in a specific pattern, a high-frequency square-wave AC signal is generated at the output of the bridge. This switching frequency is typically high, ranging from tens to hundreds of kilohertz, which helps reduce the size of the transformer and other passive components [24]. The high-frequency AC produced by the full-bridge circuit is then fed into a HFT.

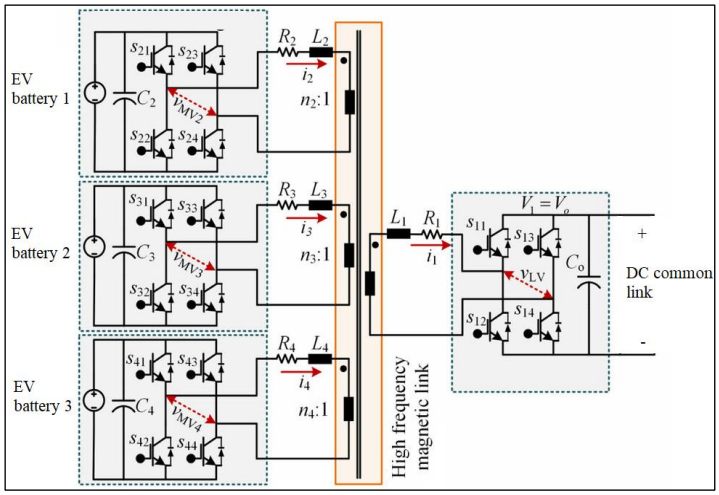

Figure 4: MAFB circuit topology for EV charging station.
Source: Authors, (2025).

Depending on the application and the turns ratio of the transformer, it can step the voltage up or down. The transformer also provides electrical isolation between the input and output, enhancing safety and noise suppression. On the secondary side of the transformer, the high-frequency AC is rectified back into DC using diodes or synchronous rectifiers. The resulting rectified output is then processed through a filtering stage, usually composed of capacitors and inductors, to smooth out any ripples and produce a stable DC output voltage.

The MAFB can be operated in both directions which can charge and discharge the EV batteries as per the requirement. During charging of the EV batteries, the mode is preferred as G2V and during discharging of EV batteries the mode is preferred as V2G. In G2V mode the power from the PV source or the battery storage module charges the EV batteries. And during V2G mode the EV batteries provide power to the local load or charge the storage battery [25].

These modes are controlled by PS-PM technique which creates phase delay in the pulses which receives power. The switching pulses of full bridge which delivers power always lead to the switching pulses of full bridge which receives power. The phase delay in the switching pulses of the receiving full bridge varies the voltage developed at the output terminals.

For higher phase delay, high voltage magnitude is generated at the output of the receiving full bridge. Therefore, by varying the phase delay of the switches, regulates the EV battery charging current [26]. The phase delay signal is generated by a phase delay regulator controller which defines the phase delay angle of the switches. The control structure of the phase delay current regulator is presented in figure 5.

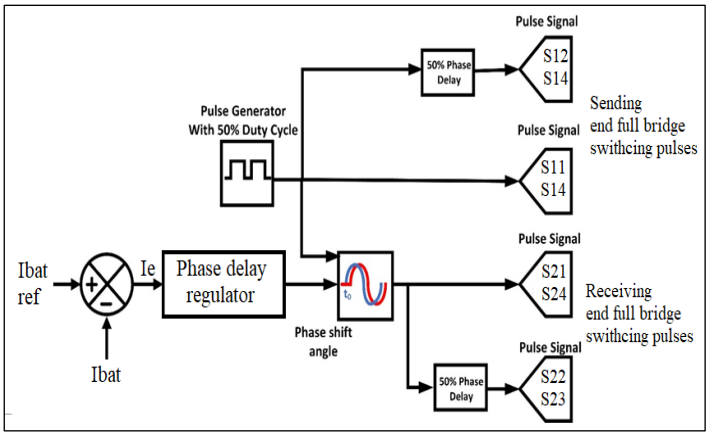

Figure 5: Phase delay regulator controller of MAFB circuit.
Source: Authors, (2025).

The controller presented in figure 5 comprises of a fixed duty ratio (50%) pulse generator producing pulses at high frequency of 20kHz. This pulse is directly fed to the sending end full bridge switches S1 S4 and with 50% phase delay to switches S2 S3. The phase shift angle for the receiving end full bridge switches is generated by the Phase delay regulator with maximum value of 90degress.

The regulator receives error current signal (Ie) by comparison of reference battery current (Ibat ref) and measured battery current (Ibat) of the EV battery pack. The Phase delay regulator is a PI controller with optimal K_{pph} and K_{iph} values which are tuned as per the current response of the EV battery pack. The phase delay signal 'Ph' is given as:

$$Ph = (Ibat\ ref - Ibat)\left(K_{pph} + \frac{K_{iph}}{s}\right) \quad (4)$$

PI controllers are not ideal for systems with rapidly changing dynamics or significant disturbances. They can experience overshoot or oscillations during transient conditions, especially if the controller gains are not tuned properly. Unlike more advanced controllers, such as PID or model-based controllers, PI controllers cannot predict future errors or anticipate changes in system behaviour.

This lack of predictive capability often results in slower response times in dynamic systems. The integral term in the PI controller accumulates error over time, which may lead to delayed corrective actions in the face of sudden disturbances. Therefore, proper tuning of the proportional (P) and integral (I) gains is essential for optimal performance. If these gains are not tuned correctly, the controller may exhibit problems such as instability, sluggishness, or excessive overshoot. Therefore, the conventional PI controller is replaced with advanced controller ANFIS

regulator for generating the phase delay angle of the receiving end full bridge switches [27].

The ANFIS is a hybrid model that merges the learning capabilities of neural networks with the reasoning abilities of fuzzy logic. It is commonly used in applications that require intelligent, adaptive, and efficient control or prediction systems. ANFIS automatically adjusts membership functions and fuzzy rules based on input-output data, which enhances its performance in dynamic or complex environments.

This system is particularly effective for modelling and controlling highly nonlinear systems, where traditional methods often struggle. During the training process, ANFIS optimizes its parameters, such as membership functions and rule weights, making it self-tuning and reducing the need for manual adjustments [27].

By integrating the interpretability of fuzzy logic with the learning capabilities of neural networks, ANFIS enhances decision-making in uncertain or ambiguous situations. The proposed ANFIS regulator comprises single input and single output variables. The input variable 'E' and output variable 'Ph' are added with seven membership functions (MFs) in each variable.

The input MFs are added with 'triangular' shape and the output MFs are constants. The input variable is set with a range of -100 to 100, considered as per the maximum and minimum error current. The phase delay Ph is set with a range from -0.0001 to 0.0001, set as the per the response of the controller. The MFs of the two variables 'E' and 'Ph' are presented in figure 6.

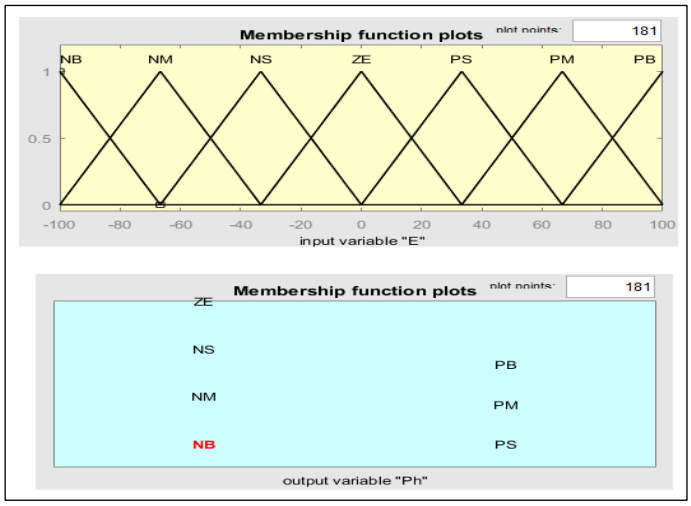

Figure 6: ANFIS variable MFs.
Source: Authors, (2025).

Each MF is defined with specific name given as per the position of the MF in the given range. On the negative side (below zero) MFs are named as NB (Negative Big), NM (Negative Medium) and NS (Negative Small). And on the positive side (above zero) are named as PS (Positive Small), Positive Medium (PM) and PB (Positive Big). However, the MF at the centre is named as ZE (Zero). Each MF convers a specific range which defines the input signals MF.

The output value is generated by rule base of the ANFIS controller given as per the requirement. The rule base used in the ANFIS modelling is 'Linear rule base' with only seven rules set as per the input and output MFs. The ANFIS is then trained using 'back propagation' optimization technique in the tool with the data provided by the input and output of the PI regulator [28]. The new trained data of the ANFIS tool can be observed in figure 7.

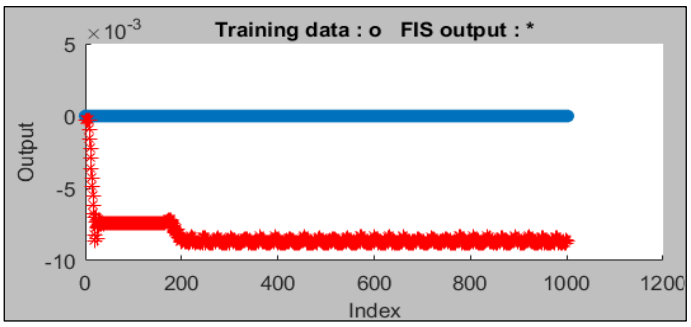

Figure 7: ANFIS trained data.
Source: Authors, (2025).

This trained ANFIS data is exported to the current regulator of the MAFB phase delay controller. The ANFIS phase delay regulator generates a stable, less oscillations phase delay signal controlling the full bridge converter with more stability. This reduces the ripple and response time of the EV battery current for the same reference signal of the controller. A comparative analysis between both the phase delay regulators (PI and ANFIS) is included in following section.

IV. SIMULATION ANALYSIS

The simulation modeling of the proposed standalone Bifacial PV array with battery backup storage module connected to local load and EV charging station in done using Simulink blocks of MATLAB software. The main blocks are taken from the Simulink library of 'Electrical' sub category and control blocks are taken from 'Continuous' and 'Signal routing' sub categories. The simulation blocks are updated as per the parameters given in table 1.

Table 1: Simulation parameters.

Name of the module	Parameters
Bifacial solar module	V_{mp} = 76.7V, I_{mp} = 5.8A, V_{oc} = 90.5V, I_{sc} = 6.21A, N_s = 4, N_p = 40, $P_{pv\ front}$ = 71.2kW, $P_{pv\ back}$= 71.2kW * 0.2 = 14.2kW, Boost converter: C_{in} = 100µF, L_b=1mH, C_{dc} = 12mF, MPPT ΔD=0.05, MPPT gain = 5, D_{int} = 0.5, fs = 5kHz.
Battery storage module	V_{nom} = 500V, Capacity = 200Ah, SOC_{int} = 90% Bidirectional converter: Lbb = 161.95µH, C_{out} = 220µF, Vdcref = 725V, Kp = 0.02, Ki = 0.0023, fc = 5kHz.
Local load	Three phase Sinusoidal inverter-controlled load = 10kW
Conventional EV charging station	C_{in} = 220µF, L_{bdc} = 161.95µH, R_{igbt} = 1mΩ, C_{out} = 0.52443mF, K_{pi} = 2, K_{ii} = 0.0023, f_{sw} = 5kHz.
MAFB EV charging station	R_{igbt} = 1mΩ, HFTF: P_n = 100kVA, f_n = 50kHz, 1:1, R_n = 0.1Ω, L_n = 2µH, R_m = 500Ω, L_m = 1mH. K_{pph} = 0.01e-6; K_{iph} = 7e-7
EV batteries	EV_1 - BMW i3 2019: Vnom = 353V, Capacity = 120Ah EV_2 - Volkawagen e-golf: Vnom=323V, Capacity = 110Ah EV_3 - Fiat 500e: Vnom = 364V, Capacity = 66Ah

Source: Authors, (2025).

With the given simulation parameters the model is updated and the simulation of the model is run with G2V and V2G modes for 1sec simulation time. The graphs of each module are presented in both operating modes of the MAFB showing the versatility of the converter. All the graphs of the voltages, currents and powers are plotted with time as reference.

The figure 8 represents the characteristics of Bifacial PV source with constant solar irradiation of 1000W/m2. The voltage of the Bifacial PV array is set at 300V and the combined currents of front and back panels is 280A. The figure 9 represents the characteristics of storage battery pack. Initially the battery storage discharges to stabilize the DC common link voltage which later on charges with the excess PV power generated. The charging of the battery is represented by negative current direction of 40A and raising SOC (State of Charge).

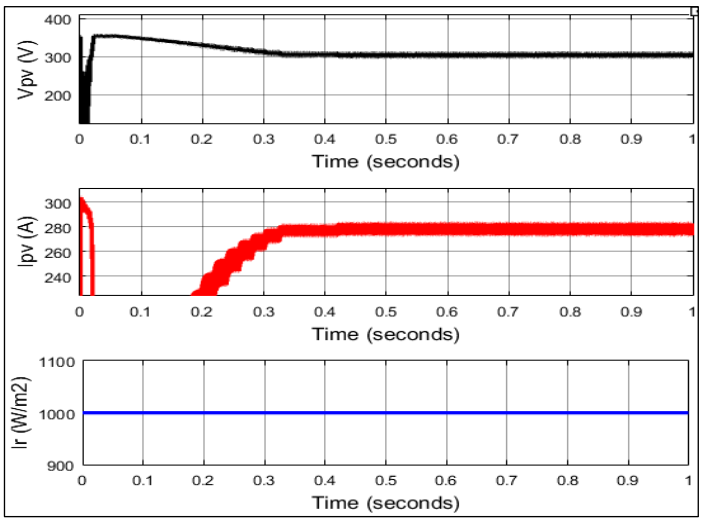

Figure 8: Bifacial PV array characteristics.
Source: Authors, (2025).

The figure 8 represents the characteristics of Bifacial PV source with constant solar irradiation of 1000W/m2. The voltage of the Bifacial PV array is set at 300V and the combined currents of front and back panels is 280A. The figure 9 represents the characteristics of storage battery pack. Initially the battery storage discharges to stabilize the DC common link voltage which later on charges with the excess PV power generated. The charging of the battery is represented by negative current direction of 40A and raising SOC (State of Charge).

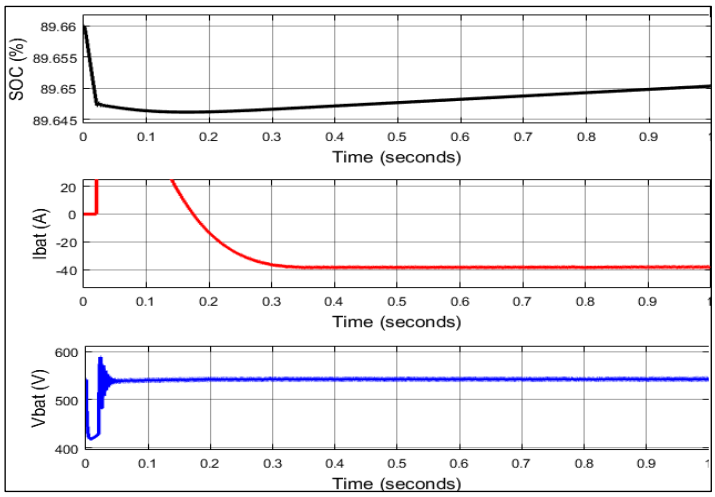

Figure9: Storage battery module characteristics during G2V mode
Source: Authors, (2025).

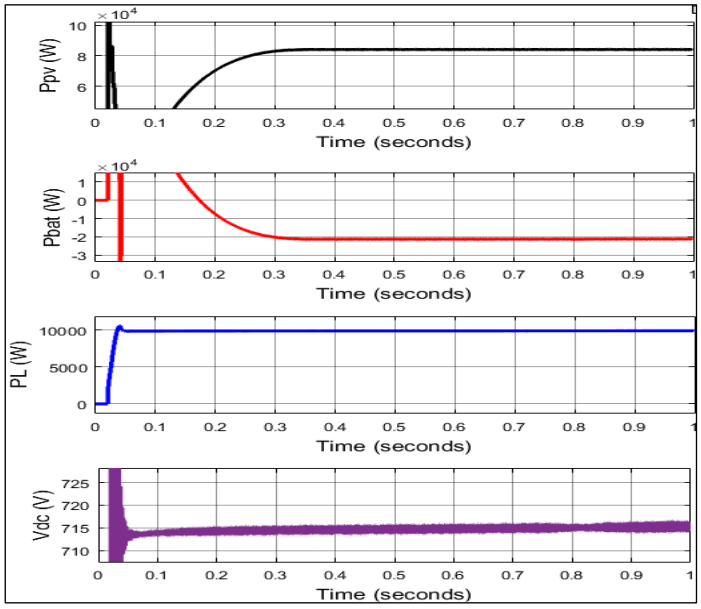

Figure 10: Active powers of Bifacial PV array, battery, load and DC common voltage during G2V

The active powers of all the modules are presented in figure 10 when the MAFB is operated in G2V mode. In this mode the power from the DC common link is transferred to the EV batteries with phase delay controller limiting the charging currents of the batteries. The total power generated by the Bifacial PV array is noted to be 82kW from which 10kW is consumed by local load, 44kW is consumed by EV charging station and the battery storage charges with 21kW.

Here, the missing 7kW is considered to be conversion loss or conduction loss of the components used in the system. The figure 11 represents the charging active powers of each EV battery connected on the secondary side of the MAFB. As per the limiting reference current set at 40A in the current controller the EV1 and EV3 battery takes 15kW, EV2 takes 14kW with a complete consumption of 44kW by the charging station.

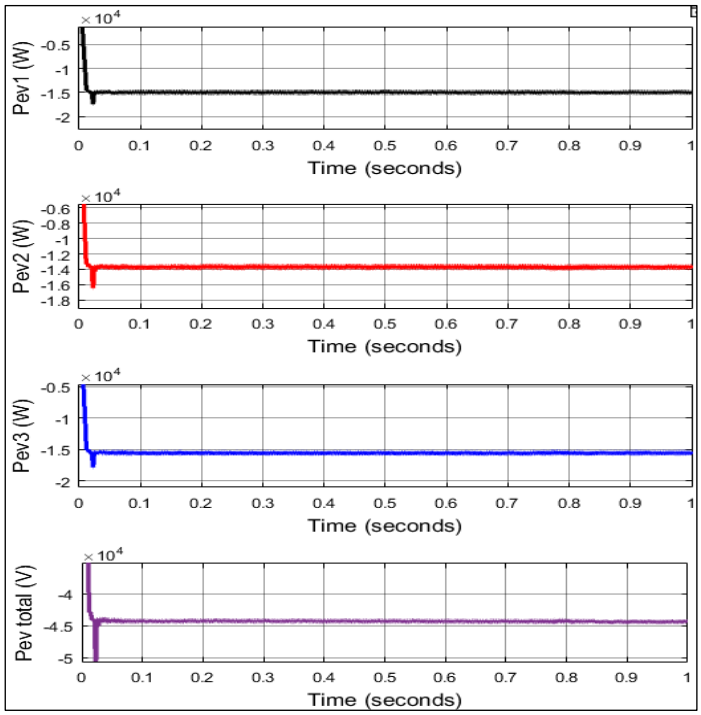

Figure 11: Active powers of EVs during G2V mode
Source: Authors, (2025).

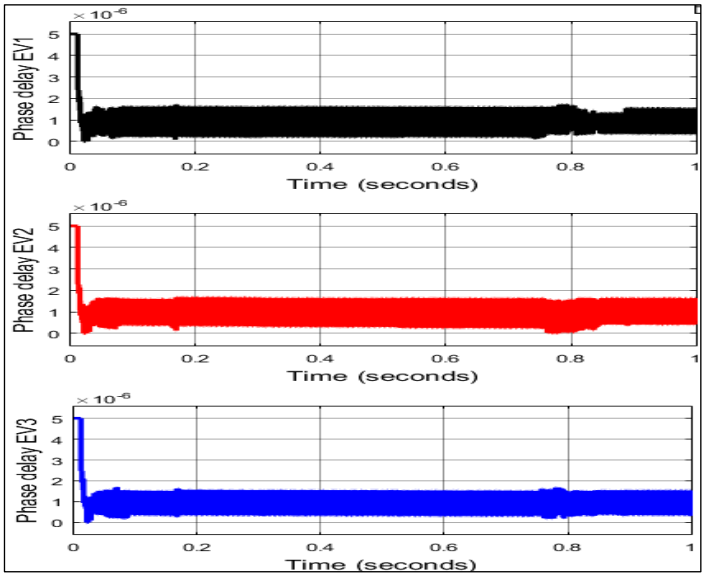

Figure 12: Phase delay time of EV full bridges switches during G2V mode.
Source: Authors, (2025).

The figure 12 shows the phase delays of each full bridge switches which is generated by the phase delay regulator controller. This time delay is caused in the pulses of the secondary bridges to ensure power consumption from the primary side winding of the HFT. In the next operating mode, the system is now operated in V2G mode where all the EVs are discharged injecting power to the battery storage module connected at the DC common link.

The figure 13 has the graphs of all the modules when operating in V2G mode. The Bifacial PV power and local load power are intact with 82kW and 10kW respectively. The battery power is increased to 140kW negative direction representing charging from PV panels and EV batteries. Adding the both the PV source power of 72kW after local load consumption and total EV charging station power of 80kW charges the battery storage with 140kW. Here, the conversion loss is 12kW in V2G mode.

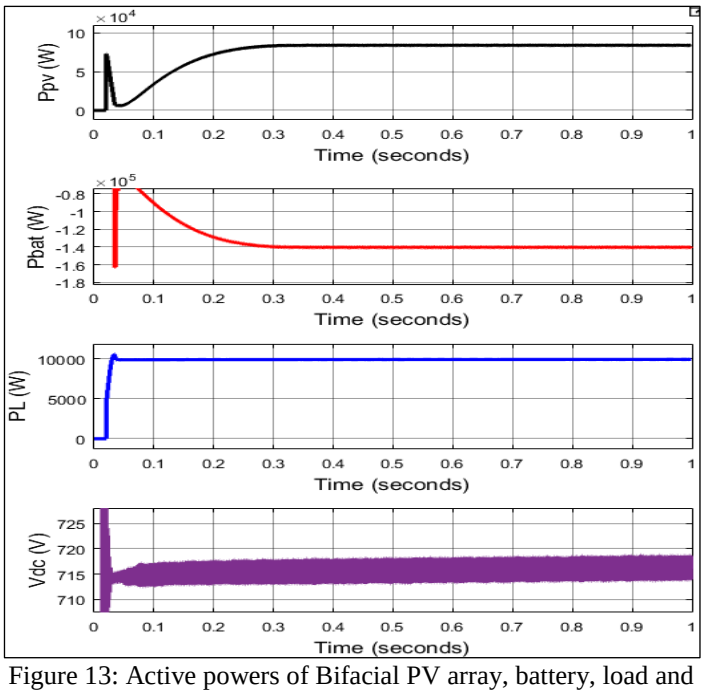

Figure 13: Active powers of Bifacial PV array, battery, load and DC common voltage during V2G.

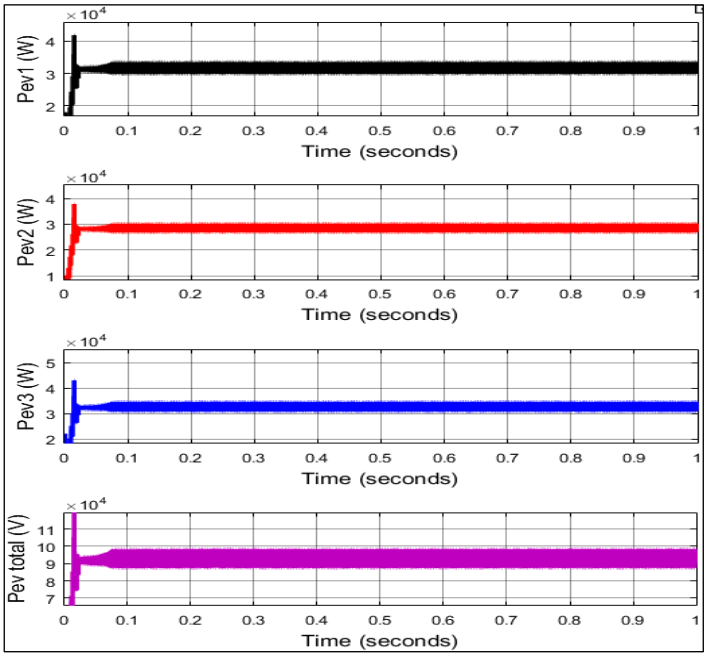

Figure 14: Active powers of EVs during V2G mode.
Source: Authors, (2025).

As per figure 14 each EV battery is discharged with powers around 30kW with a total discharge power of 90kW injected to the DC common link in V2G mode. The phase delay time generated by the phase delay regulator controller in V2G mode is presented in figure 15

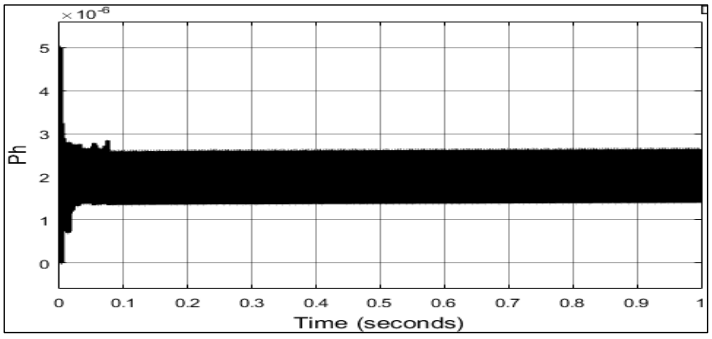

Figure 15: Phase delay time of DC common link connected full bridge during V2G mode.
Source: Authors, (2025).

The phase delay regulators are now updated with ANFIS replacing the PI controller and the simulation is run for the same ratings of the system and modes. The battery currents comparison with both the controllers can be observed in figure 16 and 17 in G2V and V2G modes respectively.

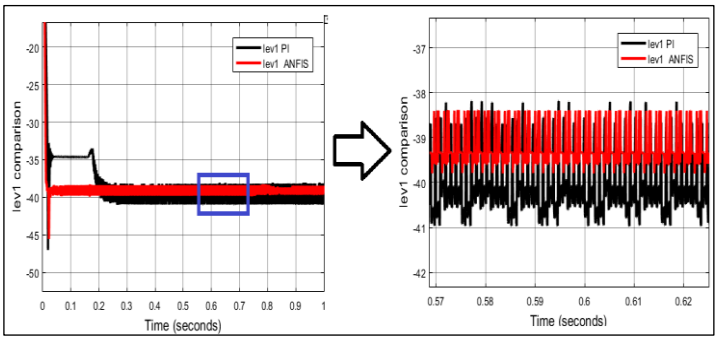

Figure 16: EV battery current comparison during G2V mode
Source: Authors, (2025).

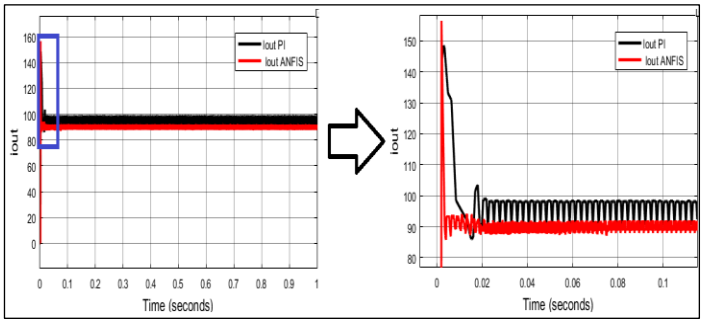

Figure 17: DC common link side full bridge output current comparison during V2G mode.
Source: Authors, (2025).

As observed from the battery current and primary full bridge currents in figure 16 and 17, the ripple and settling time are drastically reduced when the phase delay regulator is operated by ANFIS controller. This creates stability in the battery cells and the voltages of the system making it more robust to the changes occur in the circuits. The table 2 and 3 are the parametric comparison of the battery current characteristics in both operating modes G2V and V2G.

Table 2: Current characteristics comparison in G2V mode.

Name of the parameter	PI	ANFIS
Peak overshoot	47A	45A
Actual value	41A	39.5A
Settling time	0.2sec	0.03sec
Ripple	7.6%	3.8%

Source: Authors, (2025).

Table 3**:** Current characteristics comparison in V2G mode.

Name of the parameter	PI	ANFIS
Peak overshoot	150A	155A
Actual value	95A	90A
Settling time	0.02sec	0.003sec
Ripple	10.5%	3.2%

Source: Authors, (2025).

V. CONCLUSIONS

The implementation of standalone Bifacial PV source with battery storage backup connected to local AC load and EV charging station is successfully implemented. The conventional EV charging station with traditional bidirectional converter is replaced with MAFB topology with single input and multi output ports. The primary side full bridge of the MAFB is connected to DC common link where PV source, battery storage and local load are parallelly connected.

The MAFB topology has the capability to operate in both directions charging and discharging the EV batteries as per the requirement.The phase delay regulator controller of the MAFB is designed with PI regulator initially for limiting the charge and discharged currents of the EV batteries. Due to high damping of the controller more oscillations are generated in the phase delay time signal leading to higher ripple and settling time in the battery currents.

The PI controller is later replaced by ANFIS regulator for controlling the phase delay time value improving the EV battery current and full bridge current characteristics. As per the table 2 and 3 operating the MAFB with PI and ANFIS regulators in both G2V and V2G modes it is observed that there is a significant improvement in the current characteristics when operating with ANFIS controller. There is a drastic drop in ripple and settling time of the EV batteries and output current of the primary bridge when the MAFB is operated with ANFIS regulator. The current regulator can further be updated with adaptive controllers to reduce the peak overshoot and ripple content to lower values to ensure more stability of the EV battery units.

VI. AUTHOR'S CONTRIBUTION

Conceptualization: Author One, Author Two and Author Three.
Methodology: Author One and Author Two.
Investigation: Author One and Author Two, and Author Three.
Discussion of results: Author One, Author Two and Author Three.
Writing – Original Draft: Author One.
Writing – Review and Editing: Author One and Author Two.
Resources: Author Two.
Supervision: Author Two and Author Three.
Approval of the final text: Author One, Author Two and Author Three.

VII. REFERENCES

[1] Mikalai Filonchyk, Michael P. Peterson, Lifeng Zhang, Volha Hurynovich, Yi He, "Greenhouse gases emissions and global climate change: Examining the influence of CO2, CH4, and N2O," Science of The Total Environment, Volume 935, 2024, 173359, ISSN 0048-9697, https://doi.org/10.1016/j.scitotenv.2024.173359.

[2] Höök, Mikael & Tang, Xu. (2013). Depletion of fossil fuels and anthropogenic climate change - A review. Energy Policy. 53. 797-809. 10.1016/j.enpol.2012.10.046.

[3] Tonmoy Choudhury, Umar Nawaz Kayani, Azeem Gul, Syed Arslan Haider, Sareer Ahmad, "Carbon emissions, environmental distortions, and impact on growth," Energy Economics, Volume 126, 2023, 107040, ISSN 0140-9883, https://doi.org/10.1016/j.eneco.2023.107040.

[4] Osman, A.I., Chen, L., Yang, M. et al. Cost, environmental impact, and resilience of renewable energy under a changing climate: a review. Environ Chem Lett **21**, 741–764 (2023). https://doi.org/10.1007/s10311-022-01532-8

[5] Alanazi, F. Electric Vehicles: Benefits, Challenges, and Potential Solutions for Widespread Adaptation. Appl. Sci. **2023**, 13, 6016. https://doi.org/10.3390/app13106016

[6] U. N. A. Siddiqui and V. A. Kulkarni, "Grid Connected Electric Vehicle Charging Station with Multi Renewable Source," 2022 IEEE 7th International conference for Convergence in Technology (I2CT), Mumbai, India, 2022, pp. 1-5, doi: 10.1109/I2CT54291.2022.9824620.

[7] P. C. D. Goud, C. S. Nalamati and R. Gupta, "Grid Connected Renewable Energy Based EV Charger with Bidirectional AC/DC Converter," 2018 5th IEEE Uttar Pradesh Section International Conference on Electrical, Electronics and Computer Engineering (UPCON), Gorakhpur, India, 2018, pp. 1-6, doi: 10.1109/UPCON.2018.8596882.

[8] Sami Jouttijärvi, Gabriele Lobaccaro, Aleksi Kamppinen, Kati Miettunen, "Benefits of bifacial solar cells combined with low voltage power grids at high latitudes," Renewable and Sustainable Energy Reviews, Volume 161, 2022, 112354, ISSN 1364-0321, https://doi.org/10.1016/j.rser.2022.112354.

[9] Koohi, P.; Watson, A.J.; Clare, J.C.; Soeiro, T.B.; Wheeler, P.W. A Survey on Multi-Active Bridge DC-DC Converters: Power Flow Decoupling Techniques, Applications, and Challenges. Energies **2023**, 16, 5927. https://doi.org/10.3390/en16165927

[10] J. Mukhopadhyay, S. Choudhury and S. Sengupta, "ANFIS Based Speed and Current Controller for Switched Reluctance Motor," 2021 IEEE 4th International Conference on Computing, Power and Communication Technologies (GUCON), Kuala Lumpur, Malaysia, 2021, pp. 1-6, doi: 10.1109/GUCON50781.2021.9573617.

[11] Eduardo Lorenzo, "On the historical origins of bifacial PV modelling," Solar Energy, Volume 218, 2021, Pages 587-595, ISSN 0038-092X, https://doi.org/10.1016/j.solener.2021.03.006.

[12] Chraiga, Hassen Ayed. (2024). MATLAB based modeling to study the performance of bifacial solar PV system under various operating conditions .. 10.13140/RG.2.2.31357.58086.

[13] Badran, G., Dhimish, M. Comprehensive study on the efficiency of vertical bifacial photovoltaic systems: a UK case study. Sci Rep **14**, 18380 (2024). https://doi.org/10.1038/s41598-024-68018-1

[14] Debnath, Dipankar & Chatterjee, Kishore. (2015). Two-Stage Solar Photovoltaic-Based Stand-Alone Scheme Having Battery as Energy Storage Element for Rural Deployment. Industrial Electronics, IEEE Transactions on. 62. 4148-4157. 10.1109/TIE.2014.2379584.

[15] Rekha Chandola, Ashish K. Panchal, "A standalone photovoltaic energy storage application with positive pulse current battery charging," Journal of Energy Storage, Volume 85, 2024, 111184, ISSN 2352-152X, https://doi.org/10.1016/j.est.2024.111184.

[16] Javed, K.; Ashfaq, H.; Singh, R.; Hussain, S.M.S.; Ustun, T.S. Design and Performance Analysis of a Stand-alone PV System with Hybrid Energy Storage for Rural India. Electronics **2019**, 8, 952. https://doi.org/10.3390/electronics8090952

[17] Jose, Kiran & Mohammed Sulthan, Sheik & Mansoor, O.. (2022). Performance Study of Solar PV System with Bifacial PV Modules. 10.1007/978-981-19-4971-5_48.

[18] Ganesh, D. & Moorthi, Sridivya & Sudheer, H.. (2012). A Voltage Controller in Photo-Voltaic System with Battery Storage for Stand-Alone Applications. International Journal of Power Electronics and Drive Systems. 2. 9-18. 10.11591/ijpeds.v2i1.127.

[19] Jamroen, Chaowanan & Pannawan, Akekachai & Sirisukprasert, Siriroj. (2018). Battery Energy Storage System Control for Voltage Regulation in Microgrid with High Penetration of PV Generation. 1-6. 10.1109/UPEC.2018.8541888.

[20] A. K. Bhattacharjee, N. Kutkut and I. Batarseh, "Review of multiport converters for solar and energy storage integration", IEEE Trans. Power Electron., vol. 34, no. 2, pp. 1431-1445, Feb. 2019.

[21] V. Uttam and V. M. Iyer, "A Unified Modeling Approach for a Multi-Active Bridge Converter," 2022 International Power Electronics Conference (IPEC-Himeji 2022- ECCE Asia), Himeji, Japan, 2022, pp. 1614-1620, doi: 10.23919/IPEC-Himeji2022-ECCE53331.2022.9807074.

[22] S. Bandyopadhyay, P. Purgat, Z. Qin and P. Bauer, "A Multiactive Bridge Converter With Inherently Decoupled Power Flows," in IEEE Transactions on Power Electronics, vol. 36, no. 2, pp. 2231-2245, Feb. 2021, doi: 10.1109/TPEL.2020.3006266.

[23] S. Bandyopadhyay, Z. Qin and P. Bauer, "Decoupling Control of Multiactive Bridge Converters Using Linear Active Disturbance Rejection," in IEEE Transactions on Industrial Electronics, vol. 68, no. 11, pp. 10688-10698, Nov. 2021, doi: 10.1109/TIE.2020.3031531.

[24] H. Chen, Z. Hu, H. Luo, J. Qin, R. Rajagopal and H. Zhang, "Design and planning of a multiple-charger multiple-port charging system for PEV charging station", IEEE Trans. Smart Grid, vol. 10, no. 1, pp. 173-183, Jan. 2019.

[25] J. Schäfer, D. Bortis and J. W. Kolar, "Multi-port multi-cell DC/DC converter topology for electric vehicle's power distribution networks", Proc. IEEE 18th Workshop Control Model. Power Electron., pp. 1-9, 2017.

[26] Y. Chen, P. Wang, H. Li and M. Chen, "Power flow control in multi-active-bridge converters: Theories and applications", Proc. IEEE Appl. Power Electron. Conf. Expo., pp. 1500-1507, 2019.

[27] P. Mitra, S. Maulik, S. P. Chowdhury and S. Chowdhury, "ANFIS Based Automatic Voltage Regulator with Hybrid Learning Algorithm," 2007 42nd International Universities Power Engineering Conference, Brighton, UK, 2007, pp. 397-401, doi: 10.1109/UPEC.2007.4468980.

[28] M. Jamma, M. Akherraz and M. Barar, "ANFIS Based DC-Link Voltage Control of PWM Rectifier-Inverter System with Enhanced Dynamic Performance," IECON 2018 - 44th Annual Conference of the IEEE Industrial Electronics Society, Washington, DC, USA, 2018, pp. 2219-2224, doi: 10.1109/IECON.2018.8591620.